Computers in Biology and Medicine 107 (2019) 292–301

Contents lists available at ScienceDirect

Computers in Biology and Medicine

journal homepage: www.elsevier.com/locate/compbiomed

Effect of whole-body vibration and sitting configurations on lumbar spinal loads of vehicle occupants

Sorosh Amiri[a,*], Sadegh Naserkhaki[b], Mohamad Parnianpour[a]

[a] Department of Mechanical Engineering, Sharif University of Technology, Tehran, Iran
[b] Department of Biomedical Engineering, Science and Research Branch, Islamic Azad University, Tehran, Iran

ARTICLE INFO

Keywords:
Whole-body vibration (WBV)
Risk factor
Occupant posture
Spinal loads
Finite element (FE) model
Modified HYBRID III dummy

ABSTRACT

Whole-body vibration (WBV) has been identified as one of the serious risk factors leading to spinal disorders, particularly in professional drivers. Although the influential factors in this area have been investigated epidemiologically, finite element (FE) modeling can efficiently help us better understand the problem. In this study, a modified HYBRID III dummy FE model which was enhanced by detailed viscoelastic discs in the lumbar region was utilized to simulate the effect of WBV on lumbar spine loads. Spinal responses to the vertical sinusoidal vibrations of a generic seat were obtained and spinal injury risk factors were calculated. Effects of variation of excitation frequencies, three different seatback inclinations and four pre-defined occupant postures on the spinal loads were investigated as influential variables. Results showed that under sinusoidal loading with a frequency of 5 Hz and in a typical sitting configuration, disc forces remained in a safe range (< 1700 N) for short term. Collagen Fibers strain (< 0.3%) and intradiscal pressure (< 1.15 MPa) also indicated that the spinal loads were in a safe range. Additionally, calculating the risk factor according to ISO 2631-5 (about $R = 0.8$) confirmed the low probability of an adverse health effect due to WBV in long term. Frequency-domain analysis showed the resonance frequency to be at $f = 6.27$ Hz. Although according to ISO/CD 2631-5 standard, the occupant experienced the highest risk of injury at f = 7 Hz, it was found that spinal compression load at $f = 6$ Hz was 7.7% higher than the compression load at $f = 7$ Hz. Seatback oriented at 75° exhibited the highest risk of injury, nevertheless, maximum von-Mises stress in disc annulus was observed at 70°. In the evaluation of occupant posture, lordotic and slouching postures were compared and the latter exhibited higher stress ranges resulting in higher injury risk factor. Results of the model demonstrated its aptness to predict the spinal disc injuries in response to various vibrational loading and boundary conditions.

1. Introduction

Adverse effects of whole-body vibration on the human spine have made it of great importance to investigate. Low back pain in professional drivers due to whole-body vibrations (WBV) was reported by Bovenzi et al. [1]. Results of clinical studies indicate that exposure to WBV increases spinal loads [2], muscles fatigue [3] and disc injuries [4,5]. Professional drivers are continuously exposed to WBV, which leads to serious musculoskeletal disorders, so they are ranked second in the occupational diseases [6]. Results of a study by Kim et al. [7] on 96 professional drivers of heavy trucks showed that continuous exposure to the vibrations caused lower back injuries in several cases. Similarly, a study by Burstrom et al. [8] indicated that WBV raises the risk of spinal and sciatic pain.

The correlation between spinal disorders and internal loads of spine and external mechanical loads on subjects were investigated by Bovenzi et al. [9]. Estimation of the internal spinal loads was considered to be a direct and much more accurate tool compared to the external mechanical load approach (indirect tool) in predicting the spinal injuries. There is no doubt that an accurate estimation of the internal spinal loads during such activities is of utmost importance to prevent spinal injuries by avoiding those activities. To investigate the effective parameters in spinal injuries due to WBV, Seidel et al. [10] utilized a finite element (FE) model to predict internal spinal loads. It was shown that body mass, height and occupant postures were the determinant parameters. It was also demonstrated that posture was the most influential parameter in the vibration transmissibility. However, lack of quantitative or qualitative comparison of loading between different spinal levels was the main drawback of the study.

A 3-D multibody model of spine was presented by Valentini and Pennestri [11] for vibrational analysis. The spinal discs were simplified

* Corresponding author.
E-mail addresses: sorosh.amiri@yale.edu (S. Amiri), snkhaki@gmail.com (S. Naserkhaki), parnianpour@sharif.ir (M. Parnianpour).

https://doi.org/10.1016/j.compbiomed.2019.02.019
Received 11 August 2018; Received in revised form 3 February 2019; Accepted 20 February 2019

with axial joint constraints and the results were limited to the dynamic response of the vertebrae, while overlooking individual disc loads and the risk of disc injury. Yoganandan et al. conducted a relevant research focusing on fatigue response of the 'cervical' spine [12]. They presented an FE model with quasi-linear viscoelastic material properties for the discs and finally, non-linear fatigue response of the discs under cyclic loading with frequencies of 2 Hz and 4 Hz were reported. Guo and Fan employed a time-independent hyperelastic model (overlooking natural creep response of the discs) for the dynamic response of lumbar spine which was subjected to WBV and a compressive follower load. The results revealed a load magnification factor of 2–3, as compared to the static load [13]. Also, an FE model with hyperelastic material properties was used in a study by Schust et al. [14], which showed a strong correlation between risk factor and the external accelerations, duration of exposure to the vibrations, posture and sitting configuration. The time-independent model was unable to realistically simulate the disc creeping under repetitive loading condition.

To study the effect of WBV on the lumbar spine of seated occupants, a multibody model of human was required to perfectly simulate the vibration transmission from seat to the occupant. To this end, Cooper et al. [15] and Wolf et al. [16] utilized a HYBRID III dummy to assess vibrational characteristics of wheelchairs, making use of the dummy's multibody mechanism. Anyhow, HYBRID III, the well-known widely used dummy in numerical and experimental tests, lacks the lumbar spine soft tissues e.g. disc and ligaments. Therefore, the dummy is unable to accurately demonstrate the realistic behavior of discs under vehicle induced loads.

Studying the whole-body vibration of seated vehicle occupants requires an advanced (geometrically detailed and time-dependent) multibody model of the human body that mimics the dynamic response to the external loads. The HYBRID III dummy is potentially one the most appropriate devices for this application, however, the simplified lumbar spine is a major downside of utilizing it to evaluate the spine biomechanics. FE model of the HYBRID III dummy was initially developed and validated by Noureddine et al. [17]. However, recently, the FE model was modified to represent a more realistic behavior in the lumbar region [18].

In this study, utilizing the previously developed and validated modified FE model of the HYBRID III dummy, which possesses a detailed passive ligamentous lumbar spine with five viscoelastic discs (L1-L2 to L5-S1) [18], vibrational responses of the lumbar discs to the vehicle vibrations were obtained. Utilization of this model for WBV analysis addressed the problems associated with the previous studies in terms of modeling approach; highly detailed ligamentous lumbar spine with collagen fibers, annulus and nucleus resulted in a useful dataset for risk of injury evaluation. Additionally, in terms of material properties, addressed the drawback of the previous studies [11,15,16]; viscoelastic time-dependent discs were used in the current model instead of hyperelastic time-independent models overlooking creeping effect of discs [11,14,19]. The ultimate goal was to investigate the influence of variation of determinant parameters in WBV on the spinal responses and to assess the risk of injury due to vertical excitations (typical vibrational load in a vehicle). In this work, the modified FE model of the HYBRID III dummy sits on a generic seat. It provides the capability to study the effect of variations of different parameters such as excitation frequency, seatback inclination and occupant postures on the spinal responses. Results including disc forces, annulus and collagen fibers stress/strain and nucleus pressure were obtained directly from the FE analysis and risk factors (R) were calculated from the proposed approach defined by [ISO/CD 2631-5 2014] standard.

2. Methods and materials

Biomechanical performance of the spine was investigated via a previously validated and modified HYBRID III dummy [18]. The FE simulations were performed using LS-DYNA ® (Livermore Software Technology Corporation, Livermore, CA, USA).

2.1. Base FE model description (base model)

The base model was an enhanced FE model of modified HYBRID III dummy with a detailed viscoelastic ligamentous lumbar spine component. Details of the model and validation method can be found elsewhere [18], while here is a brief description.

The original FE model of the HYBRID III dummy was acquired from LS-DYNA® model library. Basically, the lumbar spine region of the original FE model includes a bent cylinder strengthened with a pair of axial steel cables. The modified FE model is similar to the original FE model except for the enhanced lumbar component which was replaced by a detailed viscoelastic ligamentous lumbar spine. The lumbar spine model consists of L1-S1 vertebrae and their associated discs and ligaments. Geometry and dimensions of the vertebrae were obtained from the average anthropometric data (50^{th} percentile male population) [18] and considered to be rigid bodies. The discs were created between the adjacent endplates and comprised nucleus pulposus and annulus fibrosus, both having quasi-linear viscoelastic (QLV) properties. Each annulus was reinforced with crisscross collagen lamellae fibers with non-linear stress-strain behavior. All seven ligaments of the lumbar spine were also included in the model. Table 1 comprehensively summarizes the properties of the model used in this study.

Positioning of the dummy on the seat and the relative coordinates and angles of the lumbar components were carried out according to the average MRI data by Sato et al. [20]. L1 and S1 vertebrae of the lumbar component were tied to the T12 and pelvis, respectively, resulting in a zero relative displacement.

Table 1
Properties of the osteo-ligamentous lumbar spine FE model.

Lumbar component	Part	Mechanical Properties	Mass (g)	Body Mass %	In-vitro body mass % [48]	Density	Ref.	Element type
Vertebrae	L1	Rigid	451	0.56	0.4	1.9 g/cm^3	[49]	8-node solid
	L2		436	0.54	0.4			
	L3		435	0.54	0.4			
	L4		381	0.47	0.3			
	L5		350	0.44	0.3			
Discs	Annulus matrix	Modified quasi-linear viscoelastic				1.9 g/cm^3	[50]	8-node solid
	Nucleus pulposus	Modified incompressible quasi-linear viscoelastic						
	Collagen fibers	Non-linear stress-strain curves stiffening from inner to outer lamellae				1 g/cm^3	[10]	Cable
Ligaments	7 Ligaments	Various non-linear stress-strain curves				1 g/cm^3	[51]	Cable

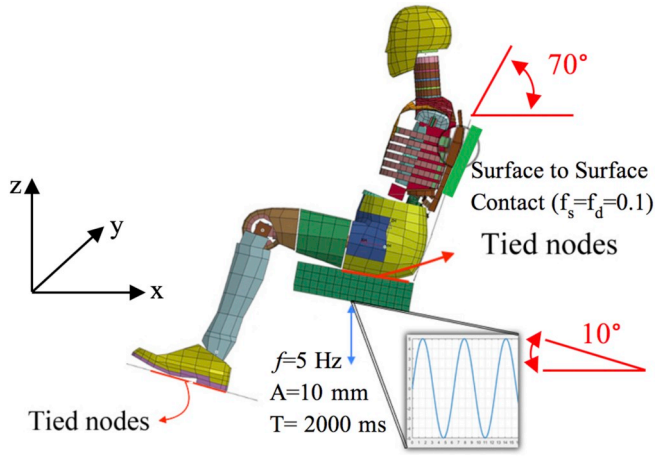

Fig. 1. An overview of the loading and boundary conditions of the base modified HYBRID III dummy FE model.

2.2. Loading and boundary conditions

Boundary and loading conditions of the model in a seated position on a rigid generic seat were illustrated in Fig. 1. A vertical sinusoidal displacement with a frequency of 5 Hz and an amplitude of 5 mm (peak to peak amplitude of 10 mm) excited the rigid seat for 2000 ms. Excitation frequency of 5 Hz was chosen to be in the midrange of the vertical vibration frequency transmitted to human lumbar spine (1–10 Hz) during driving on a typical road [21]. Amplitude of 5 mm closely lies within the range of vertical vibration protocols described in the literature [22]. Vertical excitation was applied to the seat and transmitted to the buttock of the dummy while the buttock surface nodes were tied to the seat. Pelvis was tied to the buttock, so its kinematics followed that of the buttock. Surface to surface contact was assigned between the rigid thorax and the backrest; thorax was initially in contact with the backrest and kept it with a friction coefficient of 0.1.

Weight load was applied to all parts of the model separately; the upper-body mass was about 32 kg and it was imposed on the lumbar spine through thoracic spine. Moreover, to simulate the effect of lumbar muscles, a follower load of 300 N was exerted on the lumbar spine. Local direction of the follower load was the straight line connecting centroids of each pair of adjacent vertebrae and compressed them following the path of the spine curvature.

As it was impossible to determine the exact initial geometry of the in-contact surfaces, a dynamic relaxation analysis was initially performed. Using CONTROL_DYNAMIC_RELAXATION keyword in LS-SYNA ®, by setting convergence factor to 0.001, dynamic relaxation phase was conducted. The convergence limit led to a configuration in which dissipated kinetic energy was minimized and the model reached its statically steady state.

2.3. Effect of excitation frequency

To examine the response of the model to a range of excitation frequencies, firstly, an analysis was performed with frequencies of 4–10 Hz which is the typical range of excitation in ground vehicles [23]. Secondly, time-domain analyses were performed to calculate the vibration induced spinal loads. Time-domain analyses were performed at four distinct frequencies of f = 4, 5 (base model), 6 and 7 Hz, while the sitting configurations remained unchanged.

Regarding the fact that high frequency whole body vibration improves balancing and control ability, and in order to evaluate response of the model to the higher excitation frequencies [24,25], two additional vertical vibration analyses with frequencies of f = 15 Hz and 20 Hz were performed with the same sitting configurations as well.

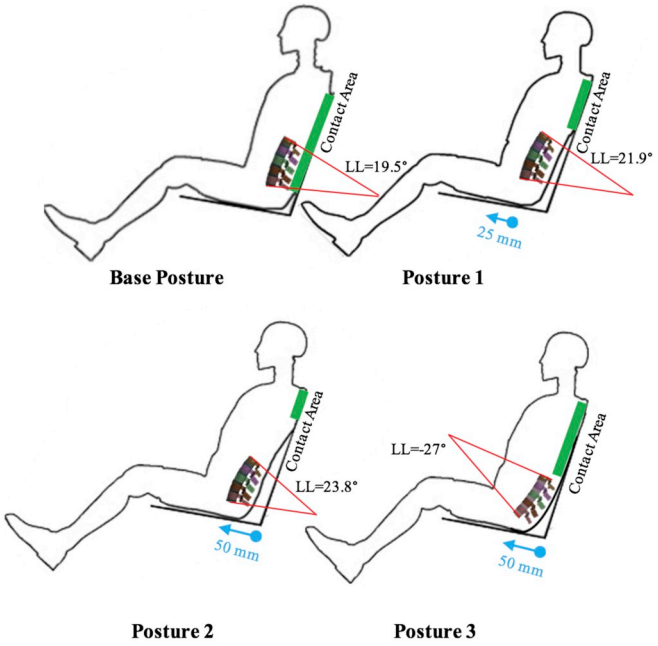

Fig. 2. Schematic illustration of occupant various postures and the corresponding Cobb angles.

2.4. Effect of backrest inclination

To study the effects of backrest angle and sitting posture, three different seatback inclination angles of 65°, 70° (base model), and 75° were investigated. Modification of the lumbar and thoracic angles were done in LS-DYNA® by adjusting the dummy repositioning module and defining local coordinate nodes at different lumbar levels to calculate the local compressive and shear loads. The lumbar angle was adjusted according to each posture and the corresponding backrest angle; thus, the contact between dummy's back and backrest was maintained in all configurations.

2.5. Effect of occupant posture

Keeping the same backrest angle, occupant was seated with three alternative postures in addition to the base posture as shown in Fig. 2. In the posture 1, the occupant's buttock was moved 25 mm anteriorly (forward along the seat pan direction); thus, pelvis and lumbar accompanied the translocation by a pelvis anterior tilt of 2° and an additional lumbar lordosis of ~2° which reduced the contact of thorax with the backrest. Similarly, in the posture 2, the buttock moved 25 mm further, which was associated with an additional pelvic tilt of 2° and further Cobb angle of ~2°. Also, a kyphotic posture, called posture 3, in which lumbar spine lost its curvature by 4° with posterior pelvic tilt of 4° was considered as a different sitting style.

2.6. Model responses

Important biomechanical parameters in the lumbar spine during WBV for analysis were the disc compressive and shear forces, von-Mises stress in annulus, intradiscal pressure and collagen fibers stress/strain. Additionally, as it was recommended in the previous studies [9], the daily disc compressive stress dose which drivers undergo within a workday was calculated and the risk factor was evaluated according to the standard ISO/CD 2631-5 2014. Due to the number of effective parameters on the problem and numerous permutations, effect of each parameter was compared only to the base model. Results of influence of each parameter on the base model were assessed separately at each vertebral level.

Risk Factor: According to ISO/CD 2631-5 2014 standard, amount of daily compressive stress on discs is calculated as follows [9]:

$$S_{ed} = \left(\sum_i S^6 \times \frac{t_d}{t_m} \right)^{1/6} (MPa) \quad (1)$$

in which S is the dynamic compressive stress due to exposure to the vibration that is defined as the sum of maximum compressive forces in each cycle on the disc cross section area. t_d is the duration of daily exposure and t_m is the duration in which S has been measured. Risk factor is defined as a measure to assess injuries due to compression stress. For a consistent pattern of vibration, Risk Factor (R) is known as follows (ISO/CD 2631-5 2014):

$$R = \left[\sum_{j=1}^{n} \left(\frac{S_{ed} \times N_j^{1/6}}{S_{uj} - C_{stat}} \right)^6 \right]^{1/6} \quad (2)$$

where S_{ed} is substituted form (1), S_{uj} is the yield stress of endplates, C_{stat} is the static compressive stress on discs resulting from body weights and occupant posture, N_j is the number of days of exposure in a year and n is the number of years of exposure. A six-hour daily driving occupation for about 15 years was assumed to be the driving habit of professional drivers with an average age of 41 years old. Assuming that all parameters were consistent within 15 years, according to Seidel et al. [10], S_u is calculated as follows:

$$S_u(MPa) = -0.067184 \times age + 6.76 \quad (3)$$

3. Results

3.1. Base model responses

Time-domain response of the compressive and shear forces were shown in Fig. 3. The highest mean compressive force of 1700 N acted on L5-S1 level while the lowest mean compressive force of 530 N on L1-L2 (Fig. 3a). The highest shear force (Fig. 3b) was observed at L5-S1 (mean force of 230 N) and it was reduced to a negligible shear force (average force of 17 N) at L3-L4 level. At this level, direction of the shear forces changed. Also, as it is clear in Fig. 3, the model experienced an initial transient response followed by a steady-state response after the second cycle with a 7% decrease in the amplitude.

Table 2 shows a complete set of maximum loads on the lumbar spine during the analysis. The von-Mises stress in the disc annulus as an indicator of injury risk was shown (Table 2) at the peak of quasi-steady response (t = 650 ms). The maximum stress increased from L1-L2 disc to L5-S1 disc. According to the stress contour (red color being the highest, blue color being the lowest stress) the absolute maximum occurred at the anterior and inferior regions of the L5-S1 disc.

Intradiscal pressure (IDP) of the discs were calculated based on the average hydrostatic pressure of all the nucleus elements. Maximum IDP showed moderate values (0.34–1.15 MPa) for different levels, indicating the highest pressure for the L5-S1 disc. For L4-L5, maximum IDP was calculated at 0.90 MPa. IDP values of *in-vivo* measurements by Wilke et al. [26] showed 0.5 MPa at L4-L5 in static back straight sitting and 0.4–0.6 MPa fluctuations while simulating a whole-body vibration task by jumping with a frequency of about $f = 1$ Hz in a seated position with the same posture. Therefore, the results indicate close correspondence to the *in-vivo* experiment.

Moreover, maximum force of the fibers in each level was observed at the outermost layers (CF_1), and maximum force was at the L5-S1 level (5.55 N). Collagen fibers stress/strain provided in Fig. 4 stated that maximum fiber strain was 0.3%, which is in a safe region according to the failure criterion of collagen fibers [27]. In fact, according to Ref. [27], for the strains of larger than 2%, collagen fibers are expected to yield, however, none of the fibers exceeded this criterion.

Also, according to Seidel et al. [10], the daily compressive stress, S_{ed}, was calculated to be 0.0053 MPa. Also, static analysis of the model indicated that C_{stat} equals 1.33 MPa; this resulted in a risk factor of 0.79 for the base model.

3.2. Effect of vibration frequency

Frequency-domain spectrum of L1 to the vertical excitations with frequencies of $f = 4$–7 Hz was depicted in Fig. 4a. The resonance frequency of the dummy model was obtained to be at $f = 6.27$ Hz at L1 which shows a $\Delta f = 2.65$ Hz shift compared to the isolated lumbar spine [18]. Effect of the resonance frequency on the responses is observed in Fig. 4b where the compressive force at L5-S1 was dramatically amplified due to the excitation frequency of $f = 6$ Hz which is the nearest frequency to the resonance point. However, disc shear force did not follow the trend of compressive force (Fig. 4c), since disc shear force at $f = 7$ Hz is larger than the other frequencies. Shear force of L5-S1 (Fig. 4c) demonstrated a faster rate of relaxation, that is to say, at $f = 7$ Hz, shear force decreased by 8.7% from the first to the last peak, however, it decreased by 5.8% for compression force relaxation.

Table 3 summarizes the effect of excitation frequency on the risk factor and annulus effective stress. Due to identical position and sitting posture of the occupant, C_{stat} is the same for all frequencies (1.33 MPa). Excitation frequencies [28–30] of 6 Hz and 7 Hz resulted in higher risk factors. At a lower excitation frequency ($f = 4$ Hz) the maximum von-Mises stress occurred at L4-L5 level, but higher excitation frequencies resulted in maximum von-Mises stress at L5-S1. Maximum von-Mises stress with excitation frequencies of $f = 6$ Hz and 7 Hz were larger than the others.

Higher excitation frequency responses ($f = 15$, 20 Hz) shown in Table 3 indicated much higher risk factors of 3.64 and 7.06 for 15 Hz and 20 Hz, respectively. Also, the von-Mises stress shown in Table 3 indicates a dramatic increase in comparison with the lower frequency excitations. At $f = 15$ Hz, maximum von-Mises stress increases by 37% compared to vibrations at $f = 7$ Hz and increases by 46% at $f = 20$ Hz, compared to $f = 15$ Hz.

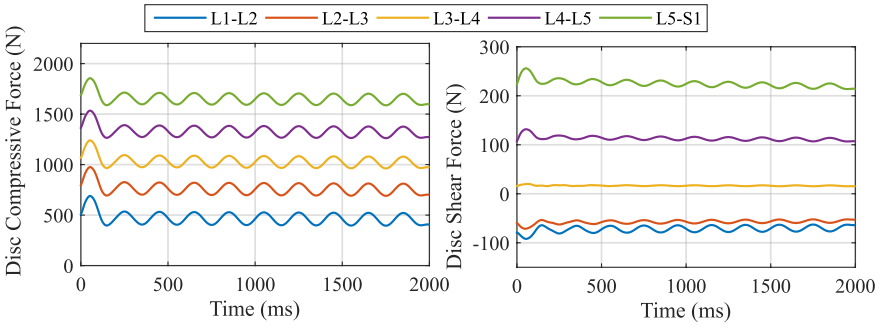

Fig. 3. Time-domain of disc force in the base model ($f = 5$ Hz), a) (left) disc compressive force, b) (right) disc shear force.

Table 2
Maximum von-Mises stress in annulus, intradiscal pressure and fibers force (CF_i corresponds to eight crisscross fibers in four lamellae, CF_1 being the outermost and CF_4 being the innermost).

von-Mises stress	Level	Maximum von-Mises stress (MPa)	Maximum intradiscal pressure (MPa)	Maximum Fibers Stress (MPa), strain %			
				CF1	CF2	CF3	CF4
	L1-L2	1.04	0.34	6.53, 0.19%	5.51, 0.15%	5.84, 0.15%	1.46, 0.14%
	L2-L3	1.18	0.50	7.13, 0.10%	5.00 0.11%	5.09 0.09%	0.97, 0.16%
	L3-L4	1.33	0.66	7.46, 0.10%	4.25, 0.09%	3.55, 0.09%	0.63, 0.20%
	L4-L5	1.51	0.90	8.16 0.14%	5.56, 0.11%	5.23 0.12%	1.74, 0.30%
	L5-S1	1.84	1.15	18.5 0.16%	10.75, 0.17%	9.53 0.12%	3.26, 0.19%

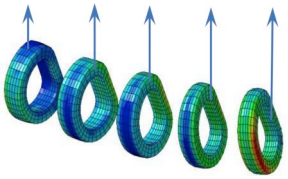

3.3. Effect of seatback inclination

Variation of disc forces (compression and shear) was shown in Fig. 5 for three seatback inclinations. The more vertically was the seatback oriented, the more compression and shear stress in the discs were observed. L5-S1 level having the largest forces experienced a 3.3% greater compression force at inclination of 75° than at 70° (base model). This effect is reversed (3.4% reduction) at an inclination of 65°. In contrast to compressive forces, disc shear forces at L5-S1 level were 5.2% larger when seatback angle reduced to 65°, whereas 16% smaller when it increased to 75°. Seatback inclination had negligible effect on the shear force at L3-L4 level.

Table 4 contains a comparison of risk factors and annulus stress in different seatback inclinations. The highest and lowest risk factors happened at 75° and 65° seatback inclinations, respectively. von-Mises stress peaked at 1.81 MPa @L4-L5 for 65° and at 1.84 MPa and 1.66 MPa @L5-S1 for 70° and 75°, respectively.

3.4. Effect of occupant posture

Influence of occupant posture on the time-domain response of disc compressive forces at all levels is depicted in Fig. 6a. It is clear that posture 2 and 3, together led to the highest compressive forces on discs (e.g. a 10% increase at L5-S1 compared to the base model), while posture 1 slightly decreased the compressive force at different levels (for instance, 4% decrease at L5-S1). Compressive forces in the posture 2 and 3 indicated very close results for L5-S1 and L4-L5. However, at the other levels, compressive force in posture 3 was somewhere between the base posture and posture 2.

The disc shear forces (Fig. 6b) also indicated that L3-L4 underwent small shear force (ranged between 20 and 50 N). The shear force was the highest at L5-S1 with a mean force of 230 N.

Due to the decrease in the lumbar lordosis in posture 3, shear forces acted oppositely compared to the other postures. In this posture the highest shear force was observed at the L4-L5. Moreover, L5-S1 and L4-L5 curves indicated shear force time-domains with opposite phases compared to L2-L3, while L3-L4 shows an almost steady force relaxation, without a significant oscillation. Such a shear force response was not previously observed in the other postures.

Risk factor corresponding to the different postures (Table 5) showed that the highest risk factor belonged to the slouching posture. In addition, the maximum von-Mises stress in the annulus for different postures (Table 5) showed that posture 3 caused the highest von-Mises stress of 2.64 MPa at L5-S1.

4. Discussion

Whole body vibration (WBV) is evidently one of the risk factors in workplaces contributing to low back pain [1,9]. Low back pain is more prevalent among drivers who are exposed to WBV, especially prolonged exposure to bus and trucks [31,32]. When subjected to the WBV, spinal responses of the modified HYBRID III dummy were investigated, and the risk of injury was assessed. Moreover, studies on the side effects of WBV indicate that long-term effects of WBV are not limited to disc degeneration, however, aftereffects of WBV showed alterations in the proprioceptive system and loss of responsiveness of the sensory system to a sudden load in subjects [33,34].

The modified HYBRID III dummy in the previous study [18] demonstrated two major enhancements which made it appropriate to the WBV analysis application. One advantage of using the modified HYBRID III dummy in whole-body vibration analysis was the viscoelastic (time-dependent) mechanical properties of the discs which enabled calculation of intradiscal pressure (IDP), disc compression/shear, collagen fibers stress/strain and annulus stress. The other advantage of using the modified dummy was its adjustable structure to study different configurations of sitting and its implications with basically no

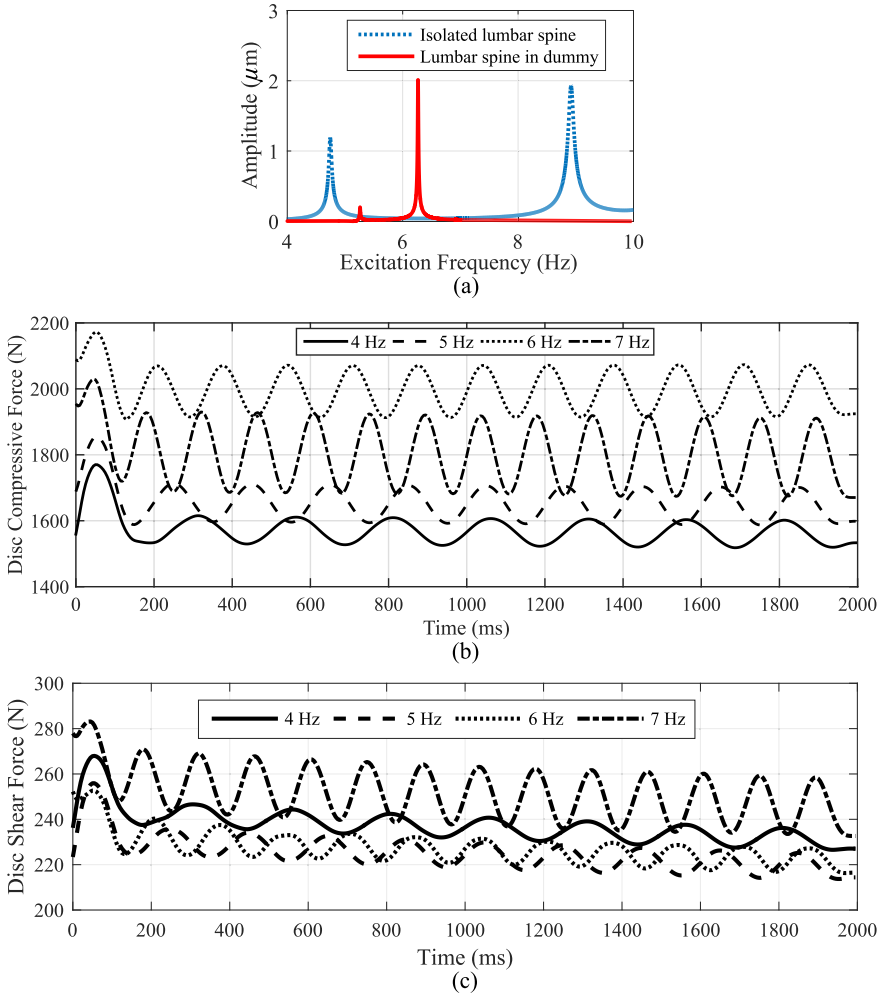

Fig. 4. (a) Frequency-domain response of the lumbar spine at L1 level compared with isolated (segregated from the dummy) lumbar spine in Ref. [18] (b) Effect of excitation frequency on L5-S1 disc compressive force (c) and shear force.

Table 3
Effect of excitation frequency on spinal responses.

Excitation frequency	4 Hz	5 Hz (Base model)	6 Hz	7 Hz	High frequency	
					15 Hz	20 Hz
$C_{stat}(MPa)$	1.33	1.33	1.33	1.33	1.33	1.33
$S_{ed}(10^{-2} \times MPa)$	0.39	0.53	0.79	0.86	2.45	4.75
Risk factor (R)	0.58	0.79	1.17	1.28	3.64	7.06
Max von-Mises stress (MPa)@ level	1.72@ L4-L5	1.84@L5-S1	2.15@ L5-S1	2.22@ L5-S1	3.05 @ L5-S1	4.46@ L5-S1

need to make a new FE geometry. Therefore, the model is able to facilitate predicting the risk of accelerated disc degeneration and vertebral injuries due to WBV over time [35–38] which was totally not obtainable from traditional dummies.

The modified HYBRID III dummy in the previous study [18] demonstrated improved results in terms of range of motions in lateral bending, head acceleration during impact (for accident analysis purposes), and overall bio-fidelity which exhibited close correspondence to the *in-vitro* and *in-vivo* experiment results.

The model revealed that vibration frequency amplified the responses and majorly increased the risk factor near the natural frequency of the dummy while the changes of seatback inclination and occupant posture in a specific range had less significant effect. The risk factor (R) provided a good insight into the influence of each parameter on the occupant safety. The risk factor was mainly used to draw a comparison between different sitting configurations and excitation frequencies, not as an absolute value to predict particular injuries. However, likelihood of injuries were particularly predicted by the level of stress/strains developed in the model.

4.1. Base model

Although WBV initially imposed a sudden load by applying a force to the motionless body, but it was transiently vanished after 140 ms. Lower spinal levels underwent relatively higher disc forces—i.e. up to 1700 N and 230 N on average, for compressive and shear components, respectively. This is not only because of more weight and follower forces, but also the applied excitation at the seat pan. Considering magnitudes of the disc forces, endplate fracture is unlikely to occur, compared to the tolerance limits [36]. However, since loads of WBV are repeated over long periods and on a daily basis, the long-term effect becomes markedly important. The ISO document (ISO/CD 2631-5 2014) considers the risk of fatigue fracture of the endplates by proposing the associated risk factor (R). Risk factors of below 0.8 and above 1.2 values are indications of low and high probability of a serious effect. Although Bovenzi et al. [9] stated that these values may be underestimated, the base model with a risk factor of 0.79 is not susceptible to a high risk.

Comparing the IDP at L4-L5 with the *in-vivo* experiment, which obtained maximum IDP of 0.6 MPa at f = 1 Hz, showed a good

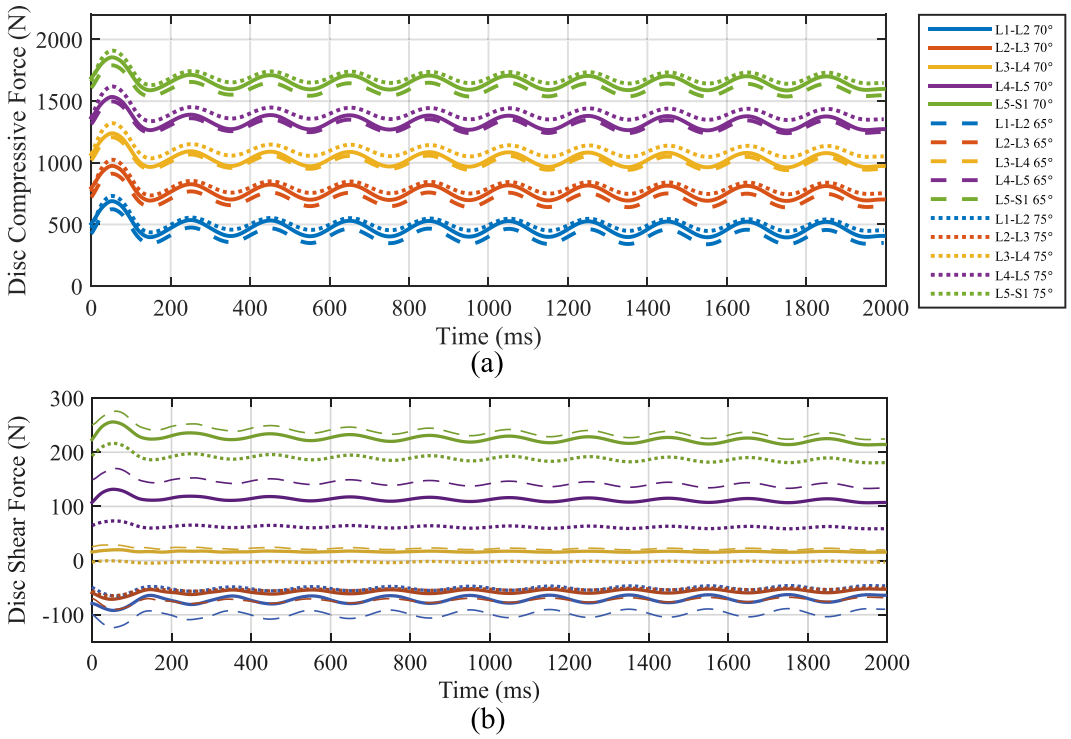

Fig. 5. Effect of seatback inclination on disc forces (a) compressive force (b) shear force.

Table 4
Effect of seatback inclination on spinal responses.

Seatback inclination	65°	70° (Base model)	75°
$C_{stat}(MPa)$	1.26	1.33	1.38
$S_{ed}(MPa \times 10^{-2})$	0.51	0.53	0.54
Risk factor (R)	0.74	0.79	0.82
Maximum von-Mises stress (MPa) @ level	1.81 @L4-L5	1.84 @L5-S1	1.66 @L5-S1

corroboration for the current model (0.9 MPa at a higher frequency of f = 5 Hz). The observed difference in the values can be explained by the different subject weights, sitting postures and higher cyclic loading frequency.

Maximum stress/strains of the collagen fibers did not exceed failure criteria of the fibers while indicated the occupant is safe by far. The most strain values were observed at CF_4 while largest stresses were observed at CF_1, which is due to the different materials properties and cross section areas at different layers.

The boundary conditions of the vibration analyses were in the range of normal WBVs induced from ground vehicles. No immediate and intense injury was observable in a relatively short time of exposure. Stresses/strains in the fibers and IDPs were in a relatively safe region, however, the risk of injury was more pronounced over prolonged exposure to such loading which is approximated by long-term analysis models such as ISO-2631-5.

4.2. Effect of vibration frequency

Resonance frequency of the lumbar spine of the modified dummy was calculated at $f = 6.27$ Hz at L1 level in z-direction (Fig. 4a). This value was lower than the isolated lumbar spine because of the lower mass associated with the isolated lumbar spine than the actual human mass due to the constraints of the *in-vitro* tests [19,39,40].

In the shear direction, the model did not show a resonant response in the shear force at the frequencies that it showed resonance in compressive forces; thus, resonance frequency of the shear direction was different from the normal direction. That is to say excitation frequency of the normal direction was ineffective in the shear direction.

Excitation frequencies of $f = 6$ Hz and 7 Hz markedly increased the L5-S1 disc compressive force by 18% (compared to base model, $f = 5$ Hz) while at $f = 4$ Hz disc compressive force decreased by 5.8% (Fig. 4b). A similar trend was expected for annulus von-Mises stresses, thus, risk factor jumped to $R = 1.17$ and $R = 1.28$ at $f = 6$ Hz and 7 Hz frequency excitations, respectively (Table 3). This indicated a higher probability of an adverse health effect due to WBV (ISO/CD 2631-5 2014).

It is noteworthy that Fig. 4b and c showed a faster rate of relaxation in shear force than the axial force which is explained by the disc material behavior; according to the quasilinear viscoelastic material used in the model [18], shear stress varies directly proportional to the time while variation of the normal stress depends on a combination of the elastic (time-independent) and viscoelastic (time-dependent) response.

From the statics point of view, load is accumulated distally and L5-S1 is expected to be the level undergoing the highest load. However, dynamic load components (normal/shear) are affected by the spine sagittal curvature and more compression may be imposed to L4-L5 level or it can make compression force on L5-S1 and L4-L5 comparable.

Interestingly, from the dynamics point of view, it was found that changing the excitation frequency not only affects the response magnitudes but also influences the mode of vibration. While the maximum von-Mises stress occurs at L5-S1 level due to excitation frequencies of 5–7 Hz, lower frequency of 4 Hz shifts the maximum von-Mises stress to be at L4-L5 level. This biomechanical justification has been confirmed by clinical observations, where both L4-L5 and L5-S1 spinal levels have been reported as the levels more susceptible to the disc degeneration, injury and pain.

Through examination of the higher frequencies, excitation frequencies of $f = 15$ Hz and $f = 20$ Hz demonstrated a dramatic increase in the risk factor, which could be explained by the softer disc response due to higher strain history accumulated during the vibrations. Number of loading cycles during such experiments was about two or three times the lower frequency excitations, therefore the strain history which is a

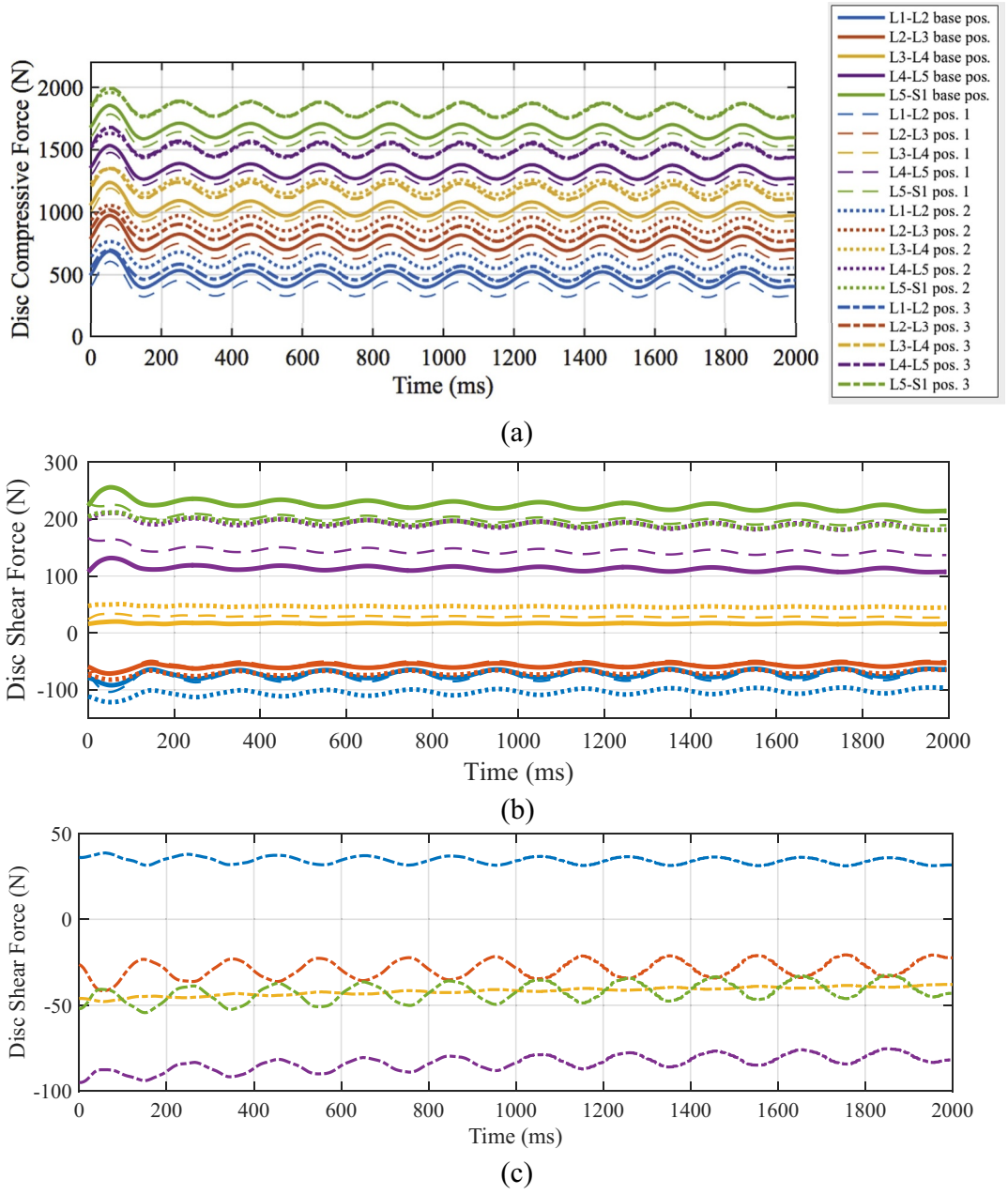

Fig. 6. Effect of occupant posture on time-domain response of compression force on discs.

Table 5
Effect of occupant posture on spinal responses.

Occupant posture	Base model	Posture (1)	Posture (2)	Posture (3)
$C_{stat}(MPa)$	1.33	1.32	1.4	1.82
$S_{ed}(MPa \times 10^{-2})$	0.53	0.51	0.59	0.58
Risk factor (R)	0.79	0.76	0.9	1.06
Maximum von-Mises stress (MPa) @level	1.84 @ L5-S1	2.12 @L5-S1	2.55 @L5-S1	2.64 @L5-S1

crucial part of the viscoelastic property recorded a larger history of strain. This dramatic increase in the risk factor is also in agreement with the *in-vivo* results which have shown that subjects undergoing WBV at high frequencies, in particular at about $f = 20$ Hz and amplitudes of larger than 0.5 mm, felt intense discomfort after the test [22].

4.3. Effect of seatback inclination

Inclination range of 65°–75° was considered as the typical range for vehicle seatback angles. A ± 5° change in the seatback slightly altered the lumbar spine responses compared to the base model (with seatback angle of 70°). Less than 5% change in disc forces could be considered as a minor effect. Disc shear force was more affected compared to the disc compression force which was due to the low-magnitude shear forces. Obviously, translation of the lumbar configuration due to change in the inclination altered the disc force components. Additionally, in the range of 65°–75°, the risk factor (on average $R = 0.78$) was small and maintained a low probability of adverse health effect due to the WBV (ISO/CD 2631-5 2014).

4.4. Effect of occupant posture

Change in the posture was feasible by alteration in the sagittal

alignment of the spine, pelvic tilt and lumbar lordosis. This also affected the contact area between the back of the dummy and the backrest. Results clearly indicated that the spinal responses were more susceptible to the changes of the posture than the seatback inclination. Previous studies also confirm the effect of body posture on spinal response due to WBV [10,14,30]. However, the effect was not deemed to be major since the risk factor remained close to the lower probability of an adverse health effect due to WBV (ISO/CD 2631-5 2014).

The opposite curvature of postures 2 and 3 developed different stress patterns in the discs. Posture 3 bore considerably higher static load at L5-S1 level, which proportionally contributed to higher dynamic loads in this posture. Also, in the posture 3 which represented a slouching posture, collagen fibers underwent a higher strain of 1.2% compared to that of posture 2 which was 0.6%; that is to say, occupants with posture 3 will be more susceptible to disc degenerations due to WBV if exposed to the excitation for long durations.

4.5. Conclusion

The advantage of the modified dummy FE model was the time-dependent behavior which enabled us to obtain time-domain response of the spine to different vibrational loading conditions. It facilitated the determination of the WBV induced forces and stress at different levels (short term effect) and then calculation of the associated risk factors (long term effect). Considering the predefined driving habit of a six-hour daily driving occupation for about 15 years, the lumbar spine was not at a high risk of injury due to WBV in the typical configuration of the base model. Change in the seatback inclination or occupant posture slightly changed the lumbar spine responses but still in the low risk range. Interestingly, posture 3 with a kyphotic lumbar curvature exhibited a higher risk factor and load values at the spinal levels compared to the other postures which corroborates the recent seat designs focusing on lumbar supports.

Although changes in the single parameters slightly altered the short-term response of the model, however, it would be expected that combination of various seatback inclinations and occupant postures would have more impact on the spinal responses. The most influential parameter was the excitation frequency which could lead to resonance of the lumbar spine responses and high risk of injury if it was close to the excitation frequency of the FE model.

4.6. Limitations

The risk factor calculated based on the ISO documents (ISO/CD 2631-5 2014) might underestimate the actual situation [9]. However, the comparison of risk factors helped us recognize and compare the different loading and boundary conditions in terms of safety. Furthermore, although the modified model made significant contributions to a well understanding of dynamics of WBV, the model is still open to more advanced considerations (e.g. considering active muscle forces) to realistically represent the human driver. Active muscles help stabilizing the spine by exerting additional force which increases the disc forces [41,42]. Once the model structure advances with multiple spinal muscles, the neural excitation pattern of muscle synergies can be included to consider both the influence of efferent and afferent neural signals on total spinal responses [43–47]. These additional factors are very complex and will replace the constant time-invariant follower-load.

Conflict of interest statement

None declared.

Funding

This research did not receive any specific grant from funding agencies in the public, commercial, or not-for-profit sectors.

References

[1] M. Bovenzi, M. Schust, M. Mauro, An overview of low back pain and occupational exposures to whole-body vibration and mechanical shocks, Med. Lav. 108 (6) (2017) 419–433.
[2] M. Fritz, Estimation of spine forces under whole-body vibration by means of a biomechanical model and transfer functions, Aviat. Space Environ. Med. 68 (6) (1997) 512–519.
[3] D.G. Wilder, A.R. Aleksiev, M.L. Magnusson, M.H. Pope, K.F. Spratt, V.K. Goel, Muscular response to sudden load: a tool to evaluate fatigue and rehabilitation, Spine 21 (22) (1996) 2628–2639.
[4] M.J. Griffin, Handbook of Human Vibration, Academic press, 2012.
[5] E. Thalheimer, Practical approach to measurement and evaluation of exposure to whole-body vibration in the workplace, Semin. Perinatol. 20 (1) (1996) 77–89 (Elsevier).
[6] B. o. L. Statistics, Nonfatal Occupational Injuries and Illnesses Requiring Days Away from Work, US Department of Labor, Bureau of Labor Statistics, Washington, DC, 2010 2011.
[7] J.H. Kim, M. Zigman, L.S. Aulck, J.A. Ibbotson, J.T. Dennerlein, P.W. Johnson, Whole body vibration exposures and health status among professional truck drivers: a cross-sectional analysis, Ann. Occup. Hyg. 60 (8) (2016) 936–948.
[8] L. Burström, T. Nilsson, J. Wahlström, Whole-body vibration and the risk of low back pain and sciatica: a systematic review and meta-analysis, Int. Arch. Occup. Environ. Health 88 (2015) 403–418.
[9] M. Bovenzi, M. Schust, G. Menzel, A. Prodi, M. Mauro, Relationships of low back outcomes to internal spinal load: a prospective cohort study of professional drivers, Int. Arch. Occup. Environ. Health 88 (4) (2015) 487–499.
[10] H. Seidel, R. Bluthner, B. Hinz, M. Schust, On the health risks of the lumbar spine due to whole-body vibration - theoretical approach, experimental data and evaluation of whole-body vibration, J. Sound Vib. (1998) 723–741 2015.
[11] P.P. Valentini, E. Pennestrì, An improved three-dimensional multibody model of the human spine for vibrational investigations, Multibody Syst. Dyn. 36 (4) (2016) 363–375.
[12] N. Yoganandan, S. Umale, B. Stemper, B. Snyder, Fatigue responses of the human cervical spine intervertebral discs, J. Mech. Behav. Biomed. Mater. 69 (2017) 30–38.
[13] L.-X. Guo, W. Fan, Dynamic response of the lumbar spine to whole-body vibration under a compressive follower preload, Spine (2017).
[14] M. Schust, et al., Measures of internal lumbar load in professional drivers–the use of a whole-body finite-element model for the evaluation of adverse health effects of multi-axis vibration, Ergonomics 58 (7) (2015) 1191–1206.
[15] R.A. Cooper, et al., Engineering better wheelchairs to enhance community participation, IEEE Trans. Neural Syst. Rehabil. Eng. 14 (4) (2006) 438–455.
[16] E.J. Wolf, C.P. DiGiovine, M.L. Ammer, Analysis of whole-body vibrations on manual wheelchairs using a Hybrid III test dummy, Proceedings of the Annual RESNA Conference, ERIC, 2001, pp. 346–348.
[17] A. Noureddine, A. Eskandarian, K. Digges, Computer modeling and validation of a hybrid III dummy for crashworthiness simulation, Math. Comput. Model. 35 (7–8) (2002) 885–893.
[18] S. Amiri, S. Naserkhaki, M. Parnianpour, Modeling and validation of a detailed FE viscoelastic lumbar spine model for vehicle occupant dummies, Comput. Biol. Med. 99 (2018) 191–200.
[19] W. Fan, L.-X. Guo, Influence of different frequencies of axial cyclic loading on time-domain vibration response of the lumbar spine: a finite element study, Comput. Biol. Med. 86 (2017) 75–81.
[20] F. Sato, et al., Analysis of the alignment of whole spine in automotive seated and supine postures using an upright open MRI system, Int. J. Automot. Eng. 7 (1) (2016) 29–35.
[21] R.-x. Fan, J. Liu, Y.-l. Li, J. Liu, J.-z. Gao, Finite element investigation of the effects of the low-frequency vibration generated by vehicle driving on the human lumbar mechanical properties, BioMed Res. Int. (2018) (2018) 9. https://doi.org/10.1155/2018/7962414 Article ID 7962414, 2314-6133, 2018.
[22] J. Kiiski, A. Heinonen, T.L. Järvinen, P. Kannus, H. Sievänen, Transmission of vertical whole body vibration to the human body, J. Bone Miner. Res. 23 (8) (2008) 1318–1325 0884-0431.
[23] W. Wang, S. Rakheja, P.-É. Boileau, Relationship between measured apparent mass and seat-to-head transmissibility responses of seated occupants exposed to vertical vibration, J. Sound Vib. 314 (3–5) (2008) 907–922.
[24] W.-H. Cheung, H.-W. Mok, L. Qin, P.-C. Sze, K.-M. Lee, K.-S. Leung, High-frequency whole-body vibration improves balancing ability in elderly women, Arch. Phys. Med. Rehabil. 88 (7) (2007) 852–857 0003-9993.
[25] D.C. Dickin, J.E. Heath, Additive effect of repeated bouts of individualized frequency whole body vibration on postural stability in young adults, J. Appl. Biomech. 30 (4) (2014) 529–533 1065-8483.
[26] H.-J. Wilke, P. Neef, B. Hinz, H. Seidel, L. Claes, Intradiscal pressure together with anthropometric data–a data set for the validation of models, Clin. Biomech. 16 (2001) S111–S126 0268-0033.
[27] J.L. Wang, M. Parnianpour, A. Shirazi-Adl, A.E. Engin, Failure criterion of collagen fiber: viscoelastic behavior simulated by using load control data, Theor. Appl. Fract. Mech. 27 (1) (1997) 1–12 0167-8442.
[28] A. Cullmann, H.P. Wölfel, Design of an active vibration dummy of sitting man, Clin. Biomech. 16 (2001) S64–S72.
[29] S. Maeda, N.J. Mansfield, Comparison of the apparent mass during exposure to

whole-body vertical vibration between Japanese subjects and ISO 5982 standard, Ind. Health 43 (3) (2005) 436–440.
[30] N. Mansfield, M.J. Griffin, Effects of posture and vibration magnitude on apparent mass and pelvis rotation during exposure to whole-body vertical vibration, J. Sound Vib. 253 (1) (2002) 93–107.
[31] R.P. Blood, M.G. Yost, J.E. Camp, R.P. Ching, Whole-body vibration exposure intervention among professional bus and truck drivers: a laboratory evaluation of seat-suspension designs, J. Occup. Environ. Hyg. 12 (6) (2015) 351–362.
[32] F. Sekkay, et al., Risk factors associated with self-reported musculoskeletal pain among short and long distance industrial gas delivery truck drivers, Appl. Ergon. 72 (2018) 69–87.
[33] Lu Li, Farhana Lamis, Sara E. Wilson, Whole-body vibration alters proprioception in the trunk, Int. J. Ind. Ergon. 38 (2008) 9–10 792-800.
[34] Robert Savage, et al., Whole-body vibration and occupational physical performance: a review, Int. Arch. Occup. Environ. Health 89 (2) (2016) 181–197.
[35] U.M. Ayturk, J.J. Garcia, C.M. Puttlitz, The micromechanical role of the annulus fibrosus components under physiological loading of the lumbar spine, J. Biomech. Eng. 132 (6) (2010) 061007 0148 0731.
[36] K. Davis, M. Parnianpour, Subject-specific compressive tolerance estimates, Technol. Health Care 11 (3) (2003) 183–193.
[37] J.C. Iatridis, I. ap Gwynn, Mechanisms for mechanical damage in the intervertebral disc annulus fibrosus, J. Biomech. 37 (8) (2004) 1165–1175 0021-9290.
[38] M. Qasim, R.N. Natarajan, H.S. An, G.B.J. Andersson, Damage accumulation location under cyclic loading in the lumbar disc shifts from inner annulus lamellae to peripheral annulus with increasing disc degeneration, J. Biomech. 47 (1) (2014) 24–31 0021-9290.
[39] L.-X. Guo, E.-C. Teo, Prediction of the modal characteristics of the human spine at resonant frequency using finite element models, Proc. IME H J. Eng. Med. 219 (4) (2005) 277–284.
[40] M. Xu, J. Yang, I. Lieberman, R. Haddas, Finite element method-based study for effect of adult degenerative scoliosis on the spinal vibration characteristics, Comput. Biol. Med. 84 (2017) 53–58.
[41] N. Arjmand, A. Shirazi-Adl, Model and in vivo studies on human trunk load partitioning and stability in isometric forward flexions, J. Biomech. 39 (3) (2006) 510–521 0021-9290.
[42] M. El-Rich, A. Shirazi-Adl, N. Arjmand, Muscle activity, internal loads, and stability of the human spine in standing postures: combined model and in vivo studies, Spine 29 (23) (2004) 2633–2642 0362-2436.
[43] E. Sedaghat-Nejad, S.J. Mousavi, M. Hadizadeh, R. Narimani, K. Khalaf, N. Campbell-Kyureghyan, M. Parnianpour, Is there a reliable and invariant set of muscle synergy during isometric biaxial trunk exertion in the sagittal and transverse planes by healthy subjects? J. Biomech. 48 (12) (2015 Sep 18) 3234–3241.
[44] B. Nasseroleslami, G. Vossoughi, M. Boroushaki, M. Parnianpour, Simulation of movement in three-dimensional musculoskeletal human lumbar spine using directional encoding-based neurocontrollers, J. Biomech. Eng. 136 (9) (2014), https://doi.org/10.1115/1.4027664 091010-091010-10.
[45] E. Rashedi, K. Khalaf, M.R. Nassajian, B. Nasseroleslami, M. Parnianpour, How does the central nervous system address the kinetic redundancy in the lumbar spine? Three-dimensional isometric exertions with 18 Hill-model-based muscle fascicles at the L4-L5 level, Proc. Inst. Mech. Eng. H 224 (3) (2010) 487–501.
[46] S. Zeinali-Davarani, A. Shirazi-Adl, B. Dariush, H. Hemami, M. Parnianpour, The effect of resistance level and stability demands on recruitment patterns and internal loading of spine in dynamic flexion and extension using a simple trunk model, Comput. Methods Biomech. Biomed. Eng. 14 (7) (2011 Jul) 645–656.
[47] A.H. Eskandari, E. Sedaghat-Nejad, E. Rashedi, A. Sedighi, N. Arjmand, M. Parnianpour, The effect of parameters of equilibrium-based 3-D biomechanical models on extracted muscle synergies during isometric lumbar exertion, J. Biomech. 49 (6) (2016 Apr 11) 967–973.
[48] D.J. Pearsall, J.G. Reid, L.A. Livingston, Segmental inertial parameters of the human trunk as determined from computed tomography, Ann. Biomed. Eng. 24 (1996) 196–210.
[49] A. Kiapour, D. Ambati, R.W. Hoy, V.K. Goel, Effect of graded facetectomy on biomechanics of Dynesys dynamic stabilization system, Spine 37 (10) (2012) E581–E589.
[50] J. Wang, M. Parnianpour, A. Shirazi-Adl, A. Engin, S. Li, A. Patwardhan, Development and validation of a viscoelastic finite element model of an L2/L3 motion segment, Theor. Appl. Fract. Mech. 28 (1) (1997) 81–93.
[51] S. Naserkhaki, N. Arjmand, A. Shirazi-Adl, F. Farahmand, M. El-Rich, Effects of eight different ligament property datasets on biomechanics of a lumbar L4-L5 finite element model, J. Biomech. 70 (2018) 33–42 https://doi.org/10.1016/j.jbiomech.2017.05.003.